

Air demand behind high head gates during emergency closure

Appel d'air derrière les hautes vannes d'amont pendant une fermeture d'urgence

ISMAIL AYDIN, *Assoc. Prof., Civil Engineering Department, Middle East Technical University, 06531 Ankara, Turkey*

ABSTRACT

Pressure drop and consecutive air demand behind high head gates during emergency closure is studied by physical and mathematical models. Measurements are done on hydraulic model of a leaf gate installed in the intake structure of a penstock. Local loss coefficients are determined as functions of Reynolds number and gate openings from measurements of discharge and piezometric levels at static positions of the gate. A mathematical model for the unsteady flow due to closing gate is formed by applying the integral continuity and energy equations on control volumes upstream and downstream of the gate. Dimensionless numbers relevant to the problem are obtained by dimensional analysis of the governing equations. Timewise variations of air discharge in the ventilation shaft and pressure behind the gate are obtained from numerical solution of the model equations. The relative air demand is computed over substantial ranges of dimensionless parameters and some design considerations are discussed.

RÉSUMÉ

La chute de pression et l'appel d'air induit derrière les vannes amont de hautes chutes pendant une fermeture d'urgence sont étudiés avec des modèles physique et mathématique. Les mesures sont réalisées sur un modèle hydraulique de vantail de vanne installé dans la prise d'eau d'une conduite d'amenée. Les pertes de charge locales sont déterminées comme fonctions du nombre de Reynolds et les ouvertures de vanne à partir des mesures de débit et des hauteurs piézométriques relevés pour des positions statiques de la vanne. Un modèle mathématique de l'écoulement instationnaire dû à la fermeture de vanne est réalisé en appliquant les équations intégrales de continuité et d'énergie aux volumes de contrôle à l'amont et à l'aval de la vanne. Les nombres sans dimension appropriés sont donnés par l'analyse dimensionnelle des équations. Les variations temporelles du débit d'air dans le puits de ventilation et de la pression derrière la vanne sont donnés par la solution numérique du modèle. L'appel d'air relatif est calculé pour une large gamme de paramètres adimensionnels et certains aspects de conception sont discutés.

1 Introduction

Leaf gates are preferred in large cross-sectioned intake and outlet structures under high heads for ordinary discharge control and emergency closure operations owing to ease in construction and maintenance. However, leaf gates may be subjected to large downpull forces and severe vibration as a result of high speed fluid around the gate lip and low pressures due to suction induced by high momentum fluid downstream of the control section (Naudascher 1991). Common application to reduce suction and adverse effects of it is aeration of the downstream face of the gate by means of ventilation shafts located immediately after the gate. From design point of view different categories of air-water flow in closed conduits may be considered depending on the mechanisms that create the air demand. In the present study, falling water surface elevation behind a high head leaf gate during emergency closure and the consequent insufflation of air and the pressure drop are investigated. As the gate is closed, water flowing into the intake from the reservoir is gradually decreased. Reduction in discharge upstream of the gate is almost synchronized with the gate motion even in emergency closures. However, deceleration of fluid downstream of the gate, where a big volume maybe flowing, is not at the same rate as the upstream, water volume in the penstock continues to flow through the turbine in the power plant by inhaling air from the ventilation shaft. Large amounts of air may enter through the ventilation shafts in a short time period to maintain volumetric continuity so as to prevent large negative pressures behind the gate.

Multicomponent, air-water, flow in a closed conduit can be classi-

fied according to the type of flow pattern (Falvey 1980). The flow patterns which develop depend on the air flowrate to water flowrate ratio, slope of the conduit and existence of a hydraulic jump. In a penstock initially water fills the whole system, flow is single component. During gate closure all types of multicomponent air-water flows may exist temporarily at certain sections, and finally after complete closure of the gate, single component flow of air starts from the gate region and continues until water is totally drained from the penstock. It is not practical and fortunately not necessary to study the specific patterns of air-water flows that may develop during gate closure for investigation of the overall air demand problem.

In the design of ventilation shaft the maximum airflow rate must be estimated first. Appropriate dimensioning and determination of the pressure drop across the shaft allows estimation of the reduced pressure acting on downstream of the gate which is an essential parameter in the analysis of the structural components which must withstand the imposed loads. The pressure downstream of the gate must be prevented from becoming too low as cavitation damage may result during prolonged periods of operation. It is not allowed but if the pressure in the water body drops below the vapor pressure of water, water column separation and rejoining may occur which induces water hammer problems. Another consequence of low pressure is increased downpull force acting on the gate, which must be added to dead weight in the design of hoisting mechanisms.

Steady state air demand has been the subject of papers by Sharma 1976, Robben and Rouve 1984, Fuentes and Garcia 1984, and Jaramillo 1988. Falvey 1968 introduces a method for time depen-

Revision received December 13, 2000. Open for discussion till August 31, 2002.

dent numerical computation of air demand using continuity and momentum equations. Time dependent measurement of air discharge is presented by Frizell 1988. Downpull forces and vibration is the main topic of papers by Naudascher 1986, de Vries 1988, and Frizell 1988. Scale effect in gate model test is discussed in detail in the symposium paper by Naudascher 1984. The monograph on air-water flow by Falvey 1980 and the design manual on hydraulic gates by Naudascher 1991 give very useful summary of theory, research and practice in related fields.

In hydraulic model studies, more than often, inclusion of all components is limited by several constraining factors. The limited space availability may be one such factor. Usually, the main point of interest is the intake, the gate and its immediate surroundings including a part of the penstock. However, in this attempt no such restriction exists. Consequently air demand simulation was made with no restriction.

The scope of the present study is to develop a mathematical model for determination of maximum air flow rate and the pressure drop during emergency closure and to perform dimensional analysis to aid estimation of prototype values to be used in the design stage. Furthermore, the mathematical model developed will also be useful in assesment of experimental results from hydraulic model studies.

2 Measurements and Analysis

2.1 Hydraulic model and measuring system

Data utilized in this study are provided from the hydraulic model of power intake structure of Birecik dam and hydroelectric power plant which is an applied research project conducted in the hydromechanics laboratory of Middle East Technical University (METU) (Göğüş et. al. 1994). The leaf gate installed in the intake structure is to be used during emergency closure operations under a water head of 41 m. Furthermore, since there is no other control mechanism between the reservoir and the turbine, the leaf gate may also function as an alternative discharge control mechanism

other than the turbine itself.

Hydraulic model constructed on 1:40 scale (Fig.1) consists of a streamlining pool to represent the reservoir, entrance details of the intake, discharge control (gate) region (section-2), ventilation shaft (section-3), transition from rectangular to circular cross-section, the penstock represented by a 0.2m diameter circular plexi-glass pipe, end valve to represent the turbine, and the discharge measuring channel. H_1 is the reservoir water surface level, h_2 is water level in the gate chamber, h_3 is piezometric head at contracted section (section-3) which is the same as water level in ventilation shaft before any air entrance and H_4 is the tailwater level. It should be noted that h_2 represents the piezometric level in the gate chamber when the gate is completely open. However, for partial openings of the gate h_2 is not simply the piezometric head at section-2 since it is affected by the overflow through the spacings between the walls of the gate chamber and the gate. This distinction is important in defining the local loss coefficients. The gate opening is indicated by e which is equal to e_0 , the tunnel height, when the gate is fully open. Discharge through the intake (upstream of section-2) is indicated by Q_1 and the discharge in the penstock downstream of the gate is indicated by Q_p . The normal operation and the maximum runaway discharges in the model scale are $0.031 \text{ m}^3/\text{s}$ and $0.041 \text{ m}^3/\text{s}$, respectively.

Water discharge in the system is measured from a triangular sharp-crested weir located at the end of the prismatic measuring channel. Water levels (H_1, h_2, h_3, H_4) are measured from the vertical scales attached on the model whereas transient pressure behind the gate (point t in Fig.1) during gate closure is measured by means of electronic pressure transducers supported by a digital data acquisition system.

2.2 Steady flow case for fully open gate

Discharge through the model, Q , water levels H_1, h_2, h_3 , and H_4 are measured to evaluate the head loss coefficients for variable openings of the end valve when the gate is fully open. Full range of discharge values ($0\sim 0.12 \text{ m}^3/\text{s}$) from closed to fully open end

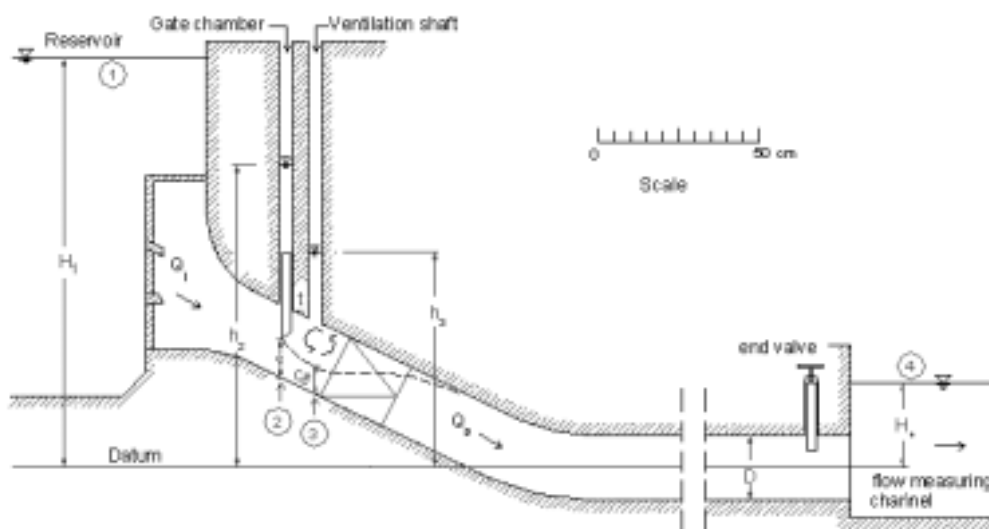


Fig.1 The hydraulic model

valve is studied. The upper bound of the range studied is much larger than the model scale maximum discharge in order to obtain a complete description of head loss coefficients as functions of Reynolds number. This is required to be able to use the findings in the assessment of the loss coefficients in prototype calculations. Reynolds number of the prototype is much larger than the Reynolds number of the model since the hydraulic model is based on Froude number similarity.

Energy equation is written between the reservoir (point-1), and the tailwater (point-4), as

$$H_1 - \Delta h_e - \Delta h_g - \Delta h_d = H_4 \quad (1)$$

where Δh_e is the entrance loss, Δh_g is the head loss mainly due to separated flows around the gate slots when the gate is fully open, Δh_d is the total head loss including friction and local losses from the gate region down to the tailwater. Above mentioned head losses are expressed as

$$\Delta h_e = H_1 - \left(h_2 + \frac{U_g^2}{2g} \right) = K_e \frac{U_g^2}{2g} \quad (2)$$

$$\Delta h_g = h_2 - h_3 = K_g \frac{U_g^2}{2g} \quad (3)$$

and rewriting (1) for Δh_d ,

$$\Delta h_d = H_1 - \Delta h_e - \Delta h_g - H_4 = K_d \frac{U_p^2}{2g} \quad (4)$$

In the above equations U_g is the average velocity of flow under the gate lip (section-2), U_p is the average flow velocity in the penstock, K_e , K_g and K_d are local loss coefficients. Equations (2) and (3) are solved for K_e and K_g respectively using the curves fitted to measured data sets (Fig.2), and the results are expressed as

$$K_e = 0.105 + \frac{44732}{R_g} \quad (5)$$

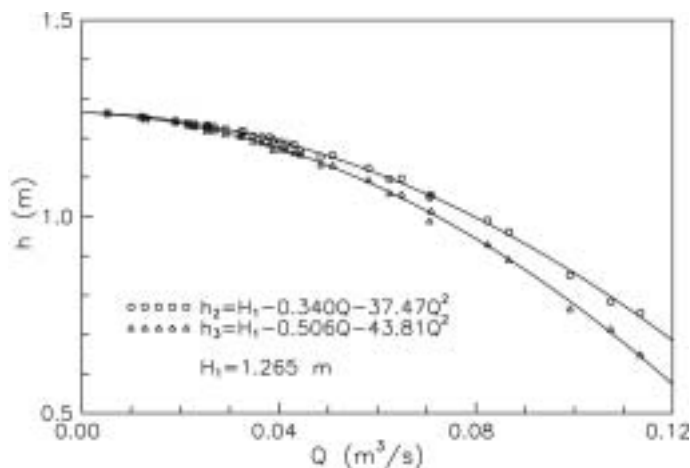


Fig.2 Measured water levels in the gate and ventilation shafts for fully open gate

$$K_g = 0.187 + \frac{21847}{R_g} \quad (6)$$

where $R_g (=D_h U_g/\nu)$ is the Reynolds number for the gate section defined by using hydraulic diameter D_h as length scale. Hydraulic diameter is defined as four times the cross-sectional area divided by the wetted perimeter. K_d is determined from (4) estimating the entrance and gate losses from (2) and (3) using (5) and (6).

$$K_d = \frac{1.0737 \times 10^{10}}{R_p^{1.696}} \quad (7)$$

where $R_p (=DU_p/\nu)$ is the Reynolds number in the penstock.

2.3 Steady flow case for partially opened gate

When the gate is lowered to reduce the discharge, flow section downstream of the gate is contracted and pressure is reduced by increased velocity. A large vortex structure recirculating on top of the contracted section is formed. In the present model the contracted section (section-3 in Fig.1) is located just under the ventilation shaft. When the Froude number at section-3 is sufficiently high, a submerged hydraulic jump is formed introducing additional energy losses. Later, as the water level in the shaft goes below the tunnel ceiling, air enters from the shaft and a free-surfaced hydraulic jump is observed. At early stages of aeration, air is well mixed with water by the hydraulic jump which occupies the whole cross section. As the gate is continued to close, air volume in the system increases, the jump moves down, and a stratified flow of air and water separated with a distinct interface develops.

Local losses around the gate should be reformulated to include the changes in flow patterns due to geometric constriction at partial gate openings. Equation (1) is modified to incorporate additional head losses.

$$H_1 - \Delta h_e - \Delta h_g - \Delta h_j - \Delta h_d = H_4 \quad (8)$$

Here, Δh_g represents local losses due to gate at partial openings, Δh_j is the head loss due to the hydraulic jump, Δh_e and Δh_d are the same as before. To determine the gate losses, energy equation can be written between the reservoir and section-3.

$$H_1 - \Delta h_e - \Delta h_g = h_3 + \frac{U_c^2}{2g} \quad (9)$$

where U_c is the average velocity of water at section-3. In this equation H_1 is fixed, h_3 and discharge are measured, Δh_e is calculated through use of equations (2) and (5), the gate loss Δh_g and the contraction coefficient C_c (used to calculate the velocity U_c) are the unknowns.

The contraction coefficient is strongly dependent on local flow conditions and the gate lip geometry (Naudascher 1984,1991). The flow depths at section-3 are measured by dye injection from the gate lip for submerged flow cases and directly measuring the

water depth for the free-surface flow cases. Measurements are given in Fig.3 in terms of contraction coefficient C_c and dimensionless gate opening, y defined as e/e_0 . In both methods the measurements are susceptible to large scale turbulent fluctuations and also to three dimensionality of the flow which makes it difficult to define a clear depth of flow section.

Gate loss coefficient for partial gate openings can be defined similar to (6)

$$K_g = K_\infty + \frac{K_R}{R_g} \quad (\text{for } 0 < y \leq 1) \quad (10)$$

However, the parameters K_∞ and K_R in equation (10) are functions of gate opening. When R_g is sufficiently large, flow is fully turbulent and K_g becomes independent of Reynolds number. K_∞ is the gate loss coefficient for a given gate opening (fixed geometry) when the Reynolds number R_g is approaching to infinity. Equation (9) is used for determination of K_∞ and K_R with measured data available. At first C_c is evaluated from flow depth measurements and fitted to a continuous curve. Five sets of h_3 data measured with different initial discharges are utilized. It is found that it is not possible to satisfy (9) for all h_3 data sets using C_c fitted to the measurements. This incompatibility is attributed to flow depth measurements for C_c and it is therefore modified, so that (9), (10) and measured h_3 data sets are all fitted. Best fitting C_c values are indicated as “estimated” shown by the continuous curve in Fig.3. Measured and estimated C_c values differ slightly only in the range where measurements are done by dye injection method. The contraction coefficient C_c and the gate loss coefficients are expressed as

$$C_c = 0.8214 - 1.308y + 7.211y^2 - 22.03y^3 + 35.06y^4 - 28.41y^5 + 9.650y^6 \quad (11.a)$$

$$K_\infty = 2.277 + 0.5997y - 26.25y^2 + 77.49y^3 - 114.2y^4 + 85.68y^5 - 25.41y^6 \quad (11.b)$$

$$K_R = 21847 \cdot \text{Exp}[-10(1-y)^8] \quad (11.c)$$

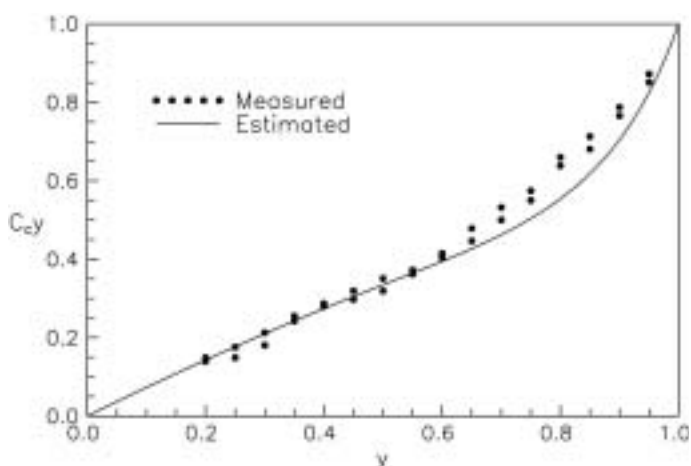


Fig.3 Flow depths at the vena contracta

Form of (11.c) is selected to fit the end conditions i.e. K_R is equal to 21847 for fully open gate as in (6), and approaches to zero as the gate is closed. The other parameters in (11.c) are obtained from numerical tests to best fit the h_3 data. Gate loss coefficients for three different initial ($y=1$) Reynolds numbers are shown in Fig.4. The continuous curve represents K_∞ which is obtained as a result of data fitting process.

Another energy loss term which appears in partial gate openings is due to the hydraulic jump downstream of the gate. By use of energy and momentum equations, expressions for the jump losses are obtained. For the free surfaced jump

$$\Delta h_j = \frac{(d - C_c e)^3}{4C_c e d} \quad (12.a)$$

and for the submerged jump

$$\Delta h_j = \frac{Q_g^2 (A_p - A_c)^2}{2g (A_p A_c)^2} \quad (12.b)$$

where d is the sequent depth given by

$$d = \frac{C_c e}{2} (\sqrt{1 + 8F_{rc}^2} - 1) \quad (12.c)$$

F_{rc} is the Froude number

$$F_{rc} = \frac{U_c}{\sqrt{g C_c e}} \quad (12.d)$$

Q_g is the discharge under the gate lip, A_g and A_c are the cross-sectional areas of the gate section (section-2) and the contracted section (section-3), respectively. The jump loss coefficient is determined from

$$K_j = \frac{\Delta h_j}{U_c^2 / 2g} \quad (12.e)$$

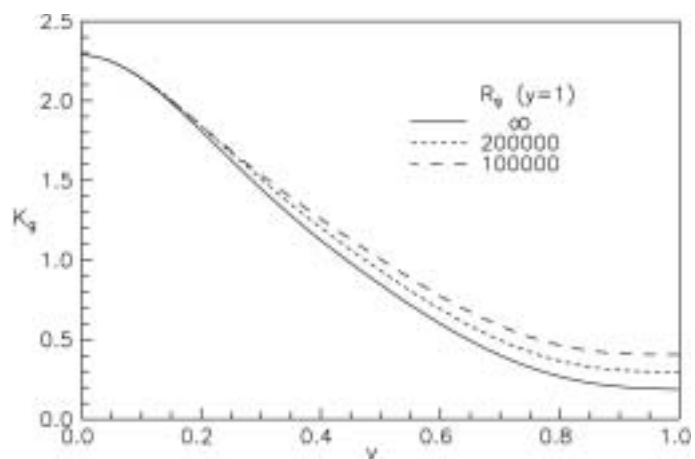


Fig.4 Gate region local loss coefficients at partial gate openings

2.4 Steady flow discharge

Discharge passing through the gate section is split into two components.

$$Q_1 = Q_g + Q_o \quad (13)$$

where Q_1 is the total discharge through the intake and Q_o is the overflow through the spacings around the gate. Overflow rate in the model is determined as

$$Q_o = 0.00202(1 - y) \quad (\text{m}^3/\text{s}) \quad (14)$$

Discharge for a given gate opening may be affected by either downstream (the end valve) or by the gate itself.

i) Downstream controlled flow:

For a given initial discharge, the gate has no control on the flow rate up to a certain gate closure, the end valve at the downstream end of the system controls the total flow rate. Equation (8) can be rewritten to calculate the flow rate under the gate lip.

$$Q_g = A_g C_d \sqrt{2g(H_1 - H_4 - \Delta h_o)} \quad (15.a)$$

where C_d is the discharge coefficient

$$C_d = \left[K_g + K_e y^2 + K_j \left(\frac{1}{C_c} \right)^2 + K_d \left(\frac{A_g}{A_p} \right)^2 \right]^{-1/2} \quad (15.b)$$

and Δh_o is the head loss in the system due to overflow component of the discharge

$$\Delta h_o = \frac{(Q_o^2 + 2Q_g Q_o)}{2g} \left(\frac{K_e}{A_t^2} + \frac{K_d}{A_p^2} \right) \quad (15.c)$$

where A_t is the cross-sectional area at the gate section for fully open gate.

ii) Gate controlled flow:

When the gate closure is enough to control the flow rate (h_3 is below the tunnel ceiling), discharge can be calculated from (9).

$$Q_g = A_g C_d \sqrt{2g(H_1 - h_3 - \Delta h_o)} \quad (16.a)$$

where

$$C_d = \left[K_g + K_e y^2 + 1/C_c^2 \right]^{-1/2} \quad (16.b)$$

and

$$\Delta h_o = \frac{(Q_o^2 + 2Q_g Q_o)}{2g} \left(\frac{K_e}{A_t^2} \right) \quad (16.c)$$

and the water level at section-3 can be written as

$$h_3 = z_3 + C_e e + d_c \quad (16.d)$$

where z_3 is channel bed elevation, d_c is the increase in water depth due to overflow which is assumed as the critical depth for Q_o ,

$$d_c = [(Q_o / w)^2 / g]^{1/3} \quad (16.e)$$

where w is the tunnel width. Comparisons of computed and measured values of discharge and the water levels (h_3) are shown in Fig.5 and Fig.6, respectively. The end valve opening, V/D , is fixed at the beginning of each experiment and the gate opening, y , is varied from 1. (fully open) to 0. (complete closure). The discharge and water levels data shown in these figures form the basis for all expressions of loss coefficients. The computed curves successfully reproduce the measurements. The model developments obtained from steady flow measurements are now utilized to study the unsteady flow cases due to closing gate.

3 Unsteady Flow Due to Closing Gate

The volume of structure between the reservoir and section-3 is called as the intake region (I), while the volume between section-3 and the end valve as the penstock region (p). Conservation of energy principle is to be applied to the intake and penstock regions to obtain the governing equations of motion of fluids; water and air. For steady flow cases, the energy equation is usually written in terms of heads which represent the energy per unit weight of the flowing fluid. Multicomponent, unsteady flow of water and air requires energy conservation written in integral forms (in terms of power) to represent the timewise energy variations in the control volumes.

3.1 Unsteady flow in the intake region

The integral energy equation is written for the intake region.

$$\frac{\partial}{\partial t} \int_I \left(\frac{U^2}{2g} + z \right) \gamma_w dV = H_1 Q_1 \gamma_w - \Delta h_e Q_1 \gamma_w - \Delta h_g Q_1 \gamma_w - H_c Q_1 \gamma_w \quad (17)$$

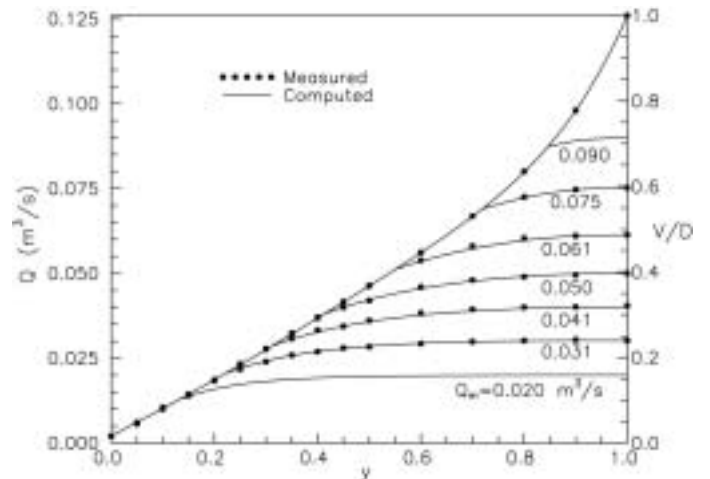


Fig.5 Comparison of computed and measured discharges

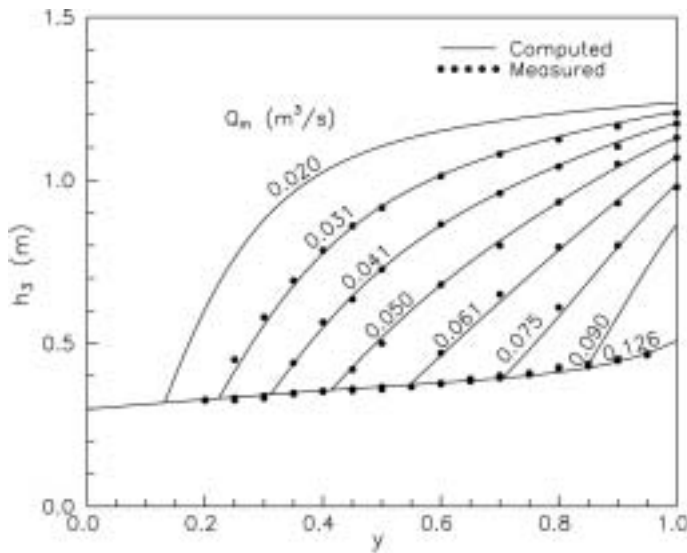


Fig.6 Comparison of computed and measured water levels in the ventilation shaft

where H_1 and H_c represent the total heads in the reservoir and in the contracted section, respectively. After substitution of head loss expressions in terms of discharges and dividing by γ_w one can write

$$\frac{S_1}{2g} \frac{\partial Q_1^2}{\partial t} = \left(H_1 - K_c \frac{Q_1^2}{2gA_i^2} - K_g \frac{Q_g^2}{2gA_g^2} - h_3 - \frac{Q_g^2}{2gA_c^2} - \frac{P_a}{\gamma_w} \right) Q_1 \quad (18)$$

where S_1 is the slenderness parameter of the intake structure defined as

$$S_1 = \int_1 \frac{dx}{A} \quad (19)$$

in which x is the axial distance, A is the cross-sectional area. P_a is the air pressure on the water surface in the ventilation shaft or in the tunnel at section-3. The elevation head, z , in the integral term in equation (17) is dropped since the intake is always full of water thus z is unvarying in time. Substituting (13) into (18)

$$\frac{S_1}{g} \frac{\partial Q_1}{\partial t} = H_1 - h_3 - \frac{P_a}{\gamma_w} - \frac{Q_1^2}{2g} \left(\frac{K_c}{A_i^2} + \frac{K_g}{A_g^2} + \frac{1}{A_c^2} \right) + \frac{(Q_o^2 + 2Q_o Q_g)}{2g} \left(\frac{K_g}{A_g^2} + \frac{1}{A_c^2} \right) \quad (20)$$

can be written. Using forward differences to express the time derivative and regrouping one obtains

$$aQ_1^2 + bQ_1 + c = 0. \quad (21.a)$$

$$a = \frac{1}{2g} \left(\frac{K_c}{A_i^2} + \frac{K_g}{A_g^2} + \frac{1}{A_c^2} \right) \quad (21.b)$$

$$b = \frac{S_1}{g\Delta t} \quad (21.c)$$

$$c = h_3 + \frac{P_a}{\gamma_w} - H_1 - \frac{S_1 Q_1^{n-1}}{g\Delta t} - \frac{(Q_o^2 + 2Q_o Q_g)}{2g} \left(\frac{K_g}{A_g^2} + \frac{1}{A_c^2} \right) \quad (21.d)$$

where $n-1$ indicates previous time level and Δt is the computational time step.

3.2 Unsteady flow in the penstock

The penstock region has two inflow sections and one outflow section. The inflows are through the gate opening and ventilation shaft. The integral energy equation for the penstock including the three active sections can be written as

$$\frac{\partial}{\partial t} \int_p \left(\frac{U^2}{2g} + z \right) \gamma_w dV = H_c Q_1 \gamma_w + H_s Q_s \gamma_s - \Delta h_j Q_1 \gamma_w - \Delta h_d Q_p \gamma_w - H_4 Q_p \gamma_w \quad (22)$$

where subscript s indicates ventilation shaft, H_s is the total head at the exit from the shaft into the penstock and Q_p is the discharge in the penstock. Initially, the ventilation shaft is filled with water therefore subscript s indicates properties of water, later as air enters into the system s indicates properties of air. Evaluating the integrals and dividing each term by γ_w one obtains

$$\frac{1}{2g} \frac{\partial}{\partial t} (Q_p^2 S_w) + \frac{\partial}{\partial t} (z_w \nabla_w) = H_c Q_1 + H_s Q_s \frac{\gamma_s}{\gamma_w} - \Delta h_j Q_1 - \frac{K_d Q_p}{2gA_p^2} Q_p^2 - H_4 Q_p \quad (23)$$

where S_w is the slenderness parameter of water filled volume of the penstock, z_w is the elevation of the centroid of the water filled volume, and ∇_w is the volume of water in the penstock. Using forward differences to express the time derivatives and regrouping one can write

$$aQ_p^2 + bQ_p + c = 0. \quad (24.a)$$

$$a = \frac{S_w}{2g\Delta t} + \frac{K_d}{2g} \frac{Q_p}{A_p^2} \quad (24.b)$$

$$b = H_4 \quad (24.c)$$

$$c = \frac{(z_w \nabla_w)^n - (z_w \nabla_w)^{n-1}}{\Delta t} + \Delta h_j Q_1 - H_c Q_1 - H_s Q_s \frac{\gamma_s}{\gamma_w} - \frac{(S_w Q_p^2)^{n-1}}{2g\Delta t} \quad (24.d)$$

During the gate closure, water volume in the intake region responds almost immediately to the gate motion, while water in the penstock responds with a time lag since the ventilation shaft supplying air volume into the penstock relieves the breaking action of the closing gate. The link between the intake and the penstock is maintained by the volumetric continuity equation written at the interface of the two volumes.

$$Q_s = Q_p - Q_1 \quad (25)$$

where Q_s is the volumetric flow rate in the ventilation shaft. Equations (21), (24) and (25) are solved iteratively starting from full gate opening to complete closure. In this iteration cycle, when the ventilation shaft discharge is evaluated, the pressure at the bottom end of the shaft can be obtained by writing the unsteady energy equation through the shaft.

$$P_s = P_a + \gamma_w \left[L_w - K_{fw} \frac{U_s^2}{2g} - \frac{L_w}{g} \frac{\partial U_s}{\partial t} \right] \quad (26.a)$$

$$P_a = -\gamma_a \left[(K_s + K_{fa} + 1) \frac{U_s^2}{2g} + \frac{L_a}{g} \frac{\partial U_s}{\partial t} \right] \quad (26.b)$$

where L_w is the length of water column in the shaft, K_{fw} is the frictional loss coefficient due to water column, K_s is the shaft entrance loss coefficient, K_{fa} is the frictional loss coefficient due to air, L_a is air filled length of the shaft and U_s is the velocity in the shaft.

3.3 Application of dimensional analysis to unsteady flow in the penstock

Before any attempt to the solution of the governing equations, dimensional analysis is performed to determine the relevant dimensionless groups. Dimensionless quantities are defined as follows:

$$Q^+ = \frac{Q}{Q_m} \quad H^+ = \frac{H}{H_m} \quad t^+ = \frac{t}{T_c} \quad \gamma_s^+ = \frac{\gamma_s}{\gamma_w} \quad (26c)$$

$$\nabla_w^+ = \frac{\nabla_w}{\nabla_p} \quad S_w^+ = \frac{S_w}{S_p} \quad z_w^+ = \frac{z_w}{z_p}$$

Subscript m refers to the initial (fully open gate) condition, H_m is the initial (maximum) total head in the penstock, Q_m is the initial (maximum) discharge in a closure operation, T_c is the closure time, z_p is the elevation of the centroid of the penstock, S_p is the

slenderness parameter of the penstock. Dimensionless form of (22) can be obtained by inserting the dimensionless parameters defined above.

$$\frac{H_r}{T_r} \frac{\partial}{\partial t^+} (Q_p^{+2} S_w^+) + \frac{1-H_r}{T_r} \frac{\partial}{\partial t^+} (z_w^+ \nabla_w^+) = H_c^+ Q_1^+ + H_s^+ Q_s^+ \gamma_s^+ - \Delta h_j^+ Q_1^+ - (\Delta h_d^+ + H_4^+) Q_p^+ \quad (27.a)$$

$$H_r = \frac{(Q_m^2 / 2g) S_p}{(Q_m^2 / 2g) S_p + z_p \nabla_p} \quad (27.b)$$

$$T_r = \frac{T_c Q_m}{\nabla_p} \quad (27.c)$$

The two dimensionless groups H_r and T_r scaling the unsteady terms in (27.a) are similarity parameters of the flow in the penstock for a given design, that is for a given set of head loss coefficients. H_r is the ratio of the initial kinetic energy to the total (kinetic+potential) energy of the fluid in the penstock. When the penstock is horizontal H_r receives the value of unity for the datum shown in Fig.1 and thus dropping the second unsteady term in (27.a). T_r is the ratio of closure time to the time necessary for a fluid particle to travel from the gate to the tailwater. For large values of T_r the fluid particles are able to travel down to the tailwater, transporting the latest dynamic properties into downstream regions and assisting the appropriate reduction in discharge. The flow rates in the intake and penstock regions are close with low inflow rate from the ventilation shaft and the case may be classified as 'slow closure'. However, when the T_r value is small the gate may close so fast that the downstream sections may receive no information about the latest dynamic properties at gate region since no fluid particle arrives and the flowrate is not adjusted properly, seeking additional volume flow from the ventilation shaft to compensate the deficiency in water discharge. This last case may be classified as 'rapid closure'.

4 Results and Discussions

The mathematical model described above is used to compute the discharges through the intake, the penstock and the ventilation shaft during emergency closure of the gate. The intake discharges for steady and unsteady cases are almost the same. The maximum difference between steady and unsteady values for $T_r=2$ is less than 1%. Therefore, for practical calculations ($T_r>2$) Q_1 can be evaluated from (15) and (16), solution of (21.a) may not be required. Although this conclusion can be generalized to all intake structures, as an exceptional case, if the slenderness parameter of the intake region, S_p , is large enough, the unsteady term in (20) is magnified and the unsteady Q_1 can be greater than steady Q_1 . The flow rates in the shaft for the normal operation discharge (0.031m³/s) and for the runaway discharge (0.041m³/s) at an emergency closure speed of $T_c=10s$ are shown in Fig.7. Until the full breaking action of the gate is applied, the discharge in the shaft is small. The maximum of the air discharge is observed near

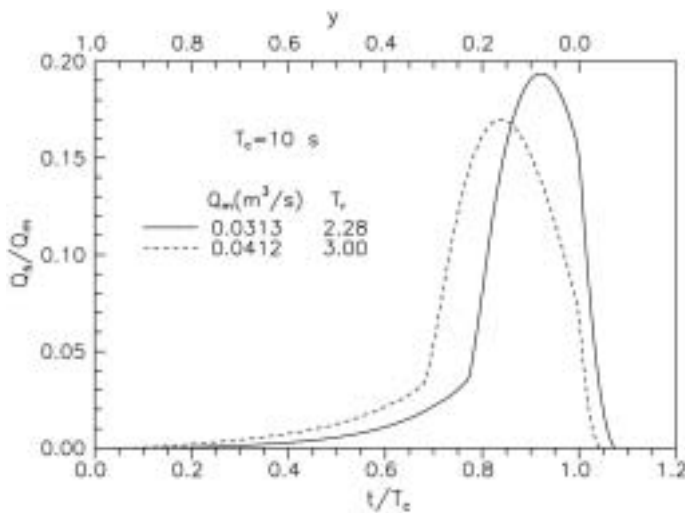


Fig.7 Timewise variation of air discharge in the ventilation shaft

the complete closure at about 8% and 16% gate openings for the normal operation and runaway discharges, respectively. When the initial discharge is large, the breaking action starts earlier (Fig.6) requiring larger maximum air discharges at an earlier stage of closure.

An example of transient pressure measured at the shaft exit (point t in Fig.1) is shown in Fig.8 together with the computed one. The difference between computed and measured values is in the range of experimental accuracy. In the unsteady measurements it is practically difficult to keep the model reservoir water level constant during the gate closure owing to finite size of the model reservoir. This results in timewise variation of H_1 value and thus affects the flowrate and the pressure. As it is seen from Fig.7 and Fig.8 computations are continued for a while after the complete closure of the gate until airflow in the system stops.

The air velocity along the centerline in the ventilation shaft is computed from the total and static head records. Measured air discharge values are obtained by integrating the power-law velocity distribution along the shaft cross-section. In the design of a ventilation shaft the maximum air discharge during the fastest closure with the maximum initial discharge in the penstock must be considered. Thus, 'air demand, Q_a ' can now be defined as the

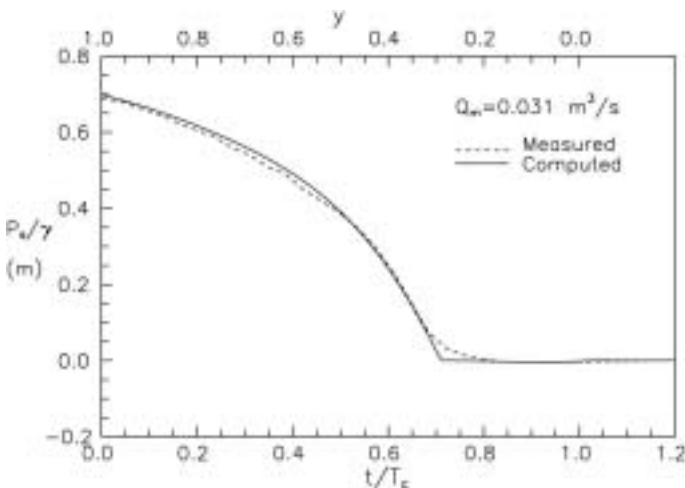


Fig.8 Pressure behind the gate

maximum air discharge observed during a closure operation. The measured and computed values of air demand and pressure drop are compared in Table.1. Experiments indicate larger air demands compared to computations which may be due to both measurement errors and limitations in modeling the loss terms in the computations.

Table 1 Comparison of measured and computed air demand and the pressure drop

Q_m (m^3/s)	T_r	H_r	Q_a/Q_m		$(P_s)_{min}/\gamma$ (mm)	
			Measured	Computed	Measured	Computed
0.0313	2.28	0.527	0.226	0.194	-3.8	-3.2
0.0412	3.00	0.658	0.197	0.169	-5.0	-4.3

Computed air demand, Q_a , normalized by the initial water discharge in the penstock, Q_m , is given in Fig.9. This chart is produced by varying the closure speed, T_c , only for the two initial (normal operation and runaway) discharges corresponding to H_r values of 0.527 and 0.658 respectively. It can be seen that the relative air demand Q_a/Q_m increases rapidly for $T_r < 2$.

To investigate the effect of the length of the penstock on the air demand, three different penstock lengths ($L=1, 3.4, 9.5$ m) are considered with the normal operation discharge (Fig.10). For the extreme cases of very rapid and very slow closures air demand becomes identical for all penstock lengths. However, around the critical values of $T_r=2$ air demand differs significantly for variable penstock lengths.

Air demand and the pressure drop behind the gate are affected also by the ventilation shaft dimensions. As the shaft length increases or diameter decreases the frictional losses increase. Increased friction loss results in negative pressure behind the gate with reduced air discharge. Relative air demand and the associated minimum pressure heads are shown in Fig.11 as functions of the dimensionless shaft length. L_e is effective shaft length increased to include the local losses. For $L_e/D_s > 40$ the reduction in air discharge and the associated increase in pressure drop is noticeable.

Air flow rate for the normal operation discharge computed with variable speed gate closure is shown in Fig.12. In the first half of

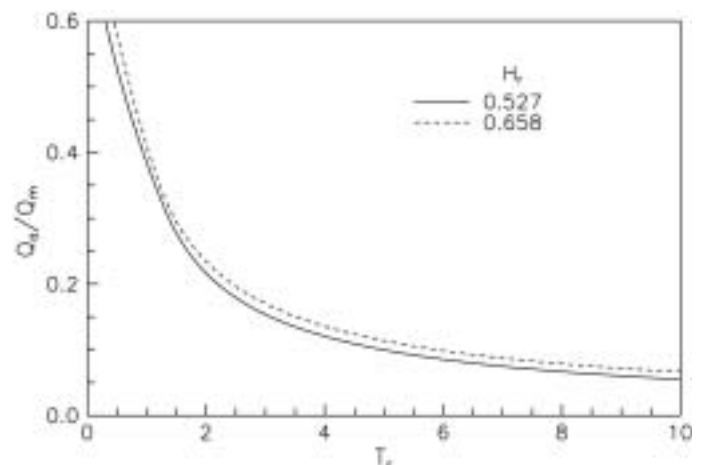


Fig.9 Air demand as function of closure speed

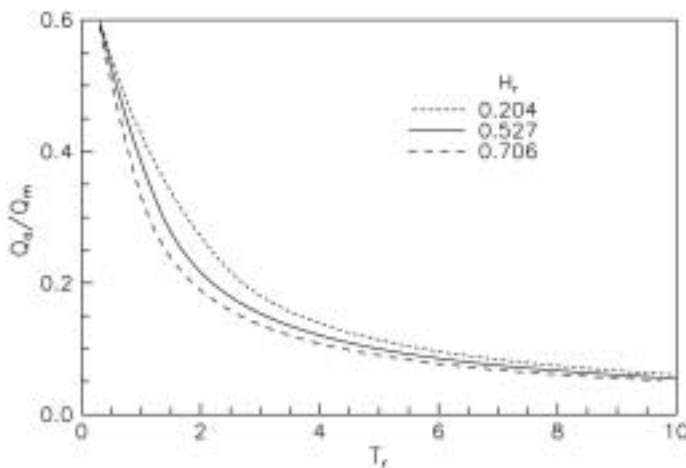


Fig.10 Air demand for different penstock lengths

the closure time, the gate moves down at high speed upto 20% opening, and in the second half time the closure speed is reduced to control the air discharge in closing the last 20% opening of the gate. Total closure time is reduced to six seconds from ten, while relative air demand is reduced to 0.154 from 0.194.

The computer program was run with the prototype data using the Reynolds dependent loss coefficients obtained from the hydraulic model. The same air demand was obtained. This is due to the fact that the maximum air flowrate is observed at gate openings less than 20% where Reynolds dependent frictional losses are negligible compared to Froude dependent losses due to hydraulic jump and the unsteady terms of (27.a). This result may also be interpreted as that the scale effect on the air demand due to different Reynolds numbers of the model and the prototype is negligible.

5 Conclusions

A mathematical model for the emergency closure of high head gates is developed to evaluate the time dependent air discharge by utilization of hydraulic model observations.

1. The dimensionless closure time T_r is a representative parameter of the speed of the gate closure and unsteady dynamics of flow

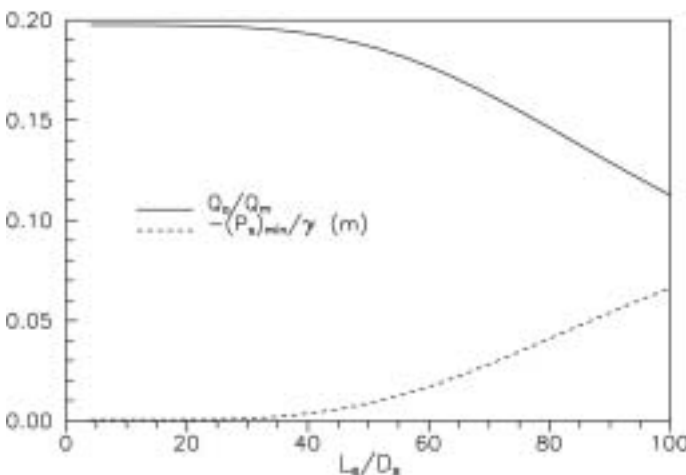


Fig.11 Air demand and the minimum pressure behind the gate for variable ventilation shaft lengths

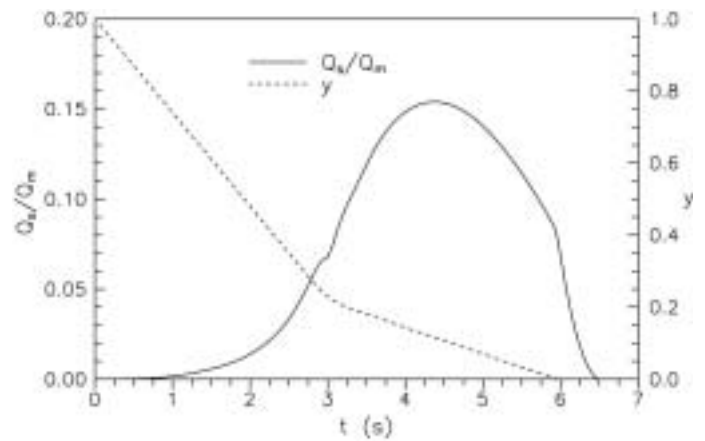


Fig.12 Air flow rate for variable speed closure

in respect to air demand.

2. Gate closure with $T_r < 2$ may be classified as rapid closure deserving special attention to air demand and the subsequent pressure drop.
3. Response of fluid in the intake region to the gate motion is almost immediate for $T_r > 2$. However, for slender and long intake geometries (large S_1) unsteady effects may be important and a time lag between the gate motion and the subsequent discharge changes can be seen.
4. Ventilation shaft length L_v/D_s must be less than 40 to keep the pressure drop insignificant.
5. Time dependent computation of air discharge and pressure drop may assist programming variable speed gate closures to reduce the closure time and the air demand simultaneously.
6. The mathematical model can be used to predict directly the prototype values however, the head loss coefficients must be known.
7. Air demand measured from hydraulic models based on Froude number similitude can be safely transformed to prototype, the scale effect is negligible.

References

- FALVEY, H.T. (1968), "Air vent computations, Morrow Point Dam", Hydraulic lab. Report HYD-584, Bureau of Reclamation, Denver, Colorado.
- FALVEY, H.T. (1980), "Air-water flow in hydraulic structures", US Department of interior, Water and Power Resources Service, Engineering monograph No.41
- FRIZELL, K. W., (1988), "Prototype tests of an emergency gate closure", Proceedings of the Int. Symposium on Model Prototype Correlation of Hydraulic Structures, ASCE, Colorado Springs, Colorado, pp.373-380
- FUENTES, R. and GARCIA, J.J., (1984), "Influence of the tunnel length on the hydraulic modelling of the air entrainment in the flow downstream of a high head gate", Symposium on Scale Effect in Modeling Hydraulic Structures, IAHR, Esslingen am Neckar, Germany, September 3-6, pp. 4.14.1-4.14.2
- GÖĞÜŞ, M., ALTINBILEK, H. D. and AYDIN, I., (1994), "Birecik dam and hydroelectric power plant intake structures hydraulic model studies", Final report, Project no:94-03-03-08, METU,

Ankara, Turkey

JARAMILLO, C. A. and VILLEGAS, F.,(1988),“Air demand of high head sluice gates: model-prototype comparison”, Proceedings of the Int. Symposium on Model Prototype Correlation of Hydraulic Structures, ASCE, Colorado Springs, Colorado, pp.95-101

NAUDASCHER, E., (1984), “Scale effects in gate model tests”, Symposium on Scale Effect in Modeling Hydraulic Structures, IAHR, Esslingen am Neckar, Germany, September 3-6, pp. 1.1.1-1.1.14

NAUDASCHER, E., (1986), “Prediction and control of downpull on tunnel gates”, J. of Hydraulic Engineering, ASCE, vol.112, No.5, pp.392-416

NAUDASCHER, E., (1991), “Hydrodynamic forces”, A. A. Balkema, Rotterdam, the Netherlands

RABBEN, L. and ROUVE, G., (1984), “Air demand of high head gates, model-family studies to quantify scale effects”, Symposium on Scale Effect in Modeling Hydraulic Structures, IAHR, Esslingen am Neckar, Germany, September 3-6, pp. 4.9.1-4.9.3

SHARMA, H. R., (1976), “Air entrainment in high head gated conduits”, J. of the Hydarulics Division, ASCE, vol.102, No.11, pp.1629-1646

DE VRIES, F.,(1988), “Model study on the emergency closure of a high head wheel gate”, Proceedings of the Int. Symposium on Model Prototype Correlation of Hydraulic Structures, ASCE, Colorado Springs, Colorado, pp.325-333

Notations

a, b, c	computational coefficients
A	cross-sectional area
A_c	cross-sectional area at the vena contracta
A_g	cross-sectional area at the gate section
A_p	cross-sectional area of the penstock
A_s	cross-sectional area of the ventilation shaft
A_t	cross-sectional area at the gate section for fully open gate
C_c	contraction coefficient
C_d	discharge coefficient
D_h	hydraulic diameter
d	sequent depth
d_c	increase in water depth due to overflow
e	gate opening
e_0	tunnel height
F_{rc}	Foude number at the vena contracta
g	gravitational acceleration
H_c	total head at the vena contracta
H_m	initial (maximum) total head in the penstock
H_r	dimensionless dynamic head
H_s	total head at the exit of the ventilation shaft
H_1	reservoir water surface elevation
H_4	tailwater level
h_2	water surface elevation in the gate chamber
h_3	water surface elevation in the ventilation shaft or at the vena contracta
K_d	energy loss coefficient for the penstock

K_e	local loss coefficient at the entrance
K_{fa}	friction loss coefficient for the air filled length of the ventilation shaft
K_{fw}	friction loss coefficient for the water filled length of the ventilation shaft
K_g	local loss coefficient at the gate section
K_j	loss coefficient for the hydraulic jump
K_s	entrance loss coefficient for the ventilation shaft
K_{∞}	local loss coefficient at the gate section for large Reynolds numbers
K_R	Reynolds dependent component of the gate loss coefficient
L_a	air filled length of the ventilation shaft
L_e	equivalent friction length of the ventilation shaft
L_w	water filled length of the ventilation shaft
P_a	air pressure on the water surface in the ventilation shaft
P_s	pressure at the exit from the ventilation shaft
Q	discharge
Q_a	air demand
Q_g	discharge under the gate lip
Q_I	discharge in the intake
Q_m	initial discharge in the intake
Q_o	overflow rate through the spacings around the gate
Q_p	discharge in the penstock
Q_s	discharge in the ventilation shaft
P_a	air pressure on the water surface in the ventilation shaft
P_s	pressure at exit of the ventilation shaft
R_g	Reynolds number at the gate section
R_p	Reynolds number in the penstock
S_I	slenderness parameter of the intake region
S_p	slenderness parameter of the penstock region
S_w	slenderness parameter of the water filled volume
t	time
T_c	closure time
T_r	dimensionless closure time
U	average velocity
U_c	average velocity at the vena contracta
U_g	average velocity at the gate section when the gate is partially open
U_p	average velocity in the penstock
U_s	average velocity in the ventilation shaft
V	end valve opening
w	tunnel width
x	axial distance
y	dimensionless gate opening (e/e_0)
z	elevation head
z_3	elevation of channel bed at section-3
z_p	elevation of centroid of the penstock
z_w	elevation of the centroid of the water filled wolume of the penstock
ν	kinematic viscosity
γ_a	specific weight of air
γ_w	specific weight of water
γ_s	specific weight of fluid in the ventilation shaft
Δh_d	total head loss in the penstock
Δh_e	head loss at the entrance

Δh_j head loss due to hydraulic jump
 Δh_g head loss at the gate section for partially open gate
 Δh_o head loss due to overflow
 Δt computational time step

∇ volume
 ∇_p volume of the penstock
 ∇_w volume of water filled portion of the penstock